Triangle mechanism in the decay process $J/\psi \to K^- K^+ a_1(1260)$

Xuan Luo, Dazhuang He, Yiling Xie, and Hao Sun*

Institute of Theoretical Physics, School of Physics, Dalian University of Technology, No. 2 Linggong Road, Dalian, Liaoning 116024, People's Republic of China

(Received 22 August 2021; accepted 21 September 2021; published 19 October 2021)

The role of the triangle mechanism in the decay process $J/\psi \to K^- K^+ a_1(1260)$ is probed. In this mechanism, a close-up resonance with mass 1823 MeV and width 122 MeV decays into $K^*\phi, K^* \to K\pi$ and then $K^*\bar{K}$ fuses into the $a_1(1260)$ resonance. We find that this mechanism leads to a triangle singularity around $M_{\rm inv}(K^- a_1(1260)) \approx 1920$ MeV, where the axial-vector meson $a_1(1260)$ is considered as a dynamically generated resonance. With the help of the triangle mechanism we find sizable branching ratios $\mathrm{Br}(J/\psi \to K^- K^+ a_1(1260), a_1 \to \pi\rho) = 1.210 \times 10^{-5}$ and $\mathrm{Br}(J/\psi \to K^- K^+ a_1(1260)) = 3.501 \times 10^{-5}$. Such an effect from the triangle mechanism of the decay process could be investigated by such as BESIII, LHCb and Belle-II experiments. This potential investigation can help us obtain the information of the axial-vector meson $a_1(1260)$.

DOI: 10.1103/PhysRevD.104.074016

I. INTRODUCTION

Researchers have shown an increased interest in triangle singularities which were first researched by Landau [1,2] in the 1960s. A considerable amount of literature [3–7] has been published on triangle singularities which are essentially brought about triangle loop Feynman diagrams where an external particle 1 decays into A and B particles, internal particle B decays into particle C and an external particle 2, and then particles A and C fuse into an external particle 3. To produce triangle singularities, according to the Coleman-Norton theorem [6], the process can occur classically and then all three intermediate particles must be put on shell and be collinear simultaneously. If there is zero width for all the internal particles, the loop integral turns out to be infinite (see e.g., [8]). Nevertheless, particle B has a finite width since it can decay to particle C and 2, which leads to a finite peak in the invariant mass distributions. This peak can be accessed in experiments. Instead of evaluating the whole amplitude of a Feynman diagram including a triangle loop, there is a more simple and practical way addressed in Ref. [9] to find the position of a triangle singularity. The condition for producing a triangle singularity is just $q_{\rm on} = q_{a\_}$, where $q_{\rm on}$ is the on-shell momentum of particle A or B in the particle 1 rest frame and $q_{a\_}$ defines one of the two solutions for the momenta of particle B when B and C are on shell to produce particle 3. Previous research [9] has established a convenient way to handle the triangle mechanism method. A considerable amount of literature has been published on the triangle mechanism. Searching for a reaction showing a peak due to the triangle singularity fails at the beginning. In 2015, the COMPASS Collaboration reported a peak at 1420 MeV for the invariant mass of the final state $\pi f_0(980)$ [10]. Soon the peak was explained as a triangle singularity corresponding to the $\pi f_0(980)$ decay mode of $a_1(1260)$ resonance [11–13]. Another consideration of the triangle mechanism lies in the abnormally enhanced isospin violating process $\eta(1405) \to \pi f_0(980)$ compared to the process $\eta(1405) \to \pi a_0(980)$ [14]. This abnormally enhancement is suggested due to the triangle singularities [15–19]. Also, to clarify an enhancement in the $K\Lambda(1405)$ invariant mass distribution of the $\gamma p \to K\Lambda(1405)$ at about $\sqrt{s} = 2110$ MeV [20], the authors of Ref. [21] tied the peak to a triangle singularity coming from a resonance $N^*(2030)$ dynamically generated from the vector-baryon interaction. In addition, there are a lot of research examples where the triangle mechanism plays an important role [22–43].

In Ref. [44], the $K^*\bar{K}$ peak related to the $a_1(1420)$ demonstrates that $f_1(1285)$ can decay into the $K^*\bar{K}$ + c.c., and there is a triangle singularity enhanced-decay mode $\pi a_0(980)$ for the $f_1(1285)$, where $f_1(1285) \to K^*\bar{K}, K^* \to \pi K$ and then $K\bar{K} \to a_0(980)$. In this paper, we focus on the reaction process $J/\psi \to K\bar{K} a_1(1260), a_1 \to \pi^+\rho^-$, where $a_1(1260)$ is viewed as a dynamically generated resonance using the chiral unitary approach [45,46], i.e., it can be described as a quasibound state of dihadron in coupled channels. The $a_1(1260)$ has been probed in the radiative decay process which is viewed as dynamically generated

*Corresponding author.
haosun@mail.ustc.edu.cn, haosun@dlut.edu.cn

hadron state [47–49]. The $a_1(1260)$ resonance is investigated in a three-body τ lepton decay process where the triangle mechanism plays a important role. Recently, the authors in Ref. [50] probe the strengths of the $a_1(1260)$ photoproduction in the $\gamma p \to a_1(1260)^+ n$ and $\gamma p \to \pi^+\pi^+\pi^- n$ reactions via the π-exchange mechanism. We reach a peak of the invariant mass $M_{\rm inv}(K^+ a_1)$ at around 1920 MeV by applying the triangle mechanism, where a close-up dynamically generated resonance decays into $K^*\phi$, $K^* \to K\pi$ and then $K^*\bar{K}$ fuses into the $a_1(1260)$ resonance. We apply the experimental data of the branching ratio of the decay $J/\psi \to \bar{K}K^*\phi$ to determine the coupling strength of the $J/\psi\bar{K}K^*\phi$ vertex. For the $a_1K^-K^{*+}$ vertex inside the triangle loop of the decay process, we apply the chiral unitary approach by viewing the $a_1(1260)$ as a dynamically generated hadron state. The branching ratio of the underlying decay process is obtained. Similarly, research [22] predicted a $f_2(1810)$ triangle singularity, coming from a nearby $f_2(1640)$ going into $K^*\bar{K}^*$, $K^* \to K\pi$, followed by $K^*\bar{K}$ fusing into $a_1(1260)$. The $J/\psi \to K\bar{K}a_1(1260)$, $a_1 \to \pi^+\rho^-$ process we suppose is a practical example of a physical process where the triangle mechanism can work. We also perform a quantitative calculation of the triangle loop amplitude t_T.

This paper has been divided into four sections. Section II deals with the calculation framework and formalism for working out the decay amplitude of $J/\psi \to K\bar{K}a_1(1260)$, $a_1 \to \pi^+\rho^-$ including the triangle mechanism. In this section, the vertex coupling involved in the tree-level process $J/\psi \to K^*\bar{K}\phi$ has been calculated where we have introduced a dynamically-generated resonance propagator. In Sec. III we give out the numerical results related to the triangle singularity around 1920 MeV and then make a discussion about them. Also, the corresponding decay branching ratios have been obtained. We reach our conclusion in Sec. IV.

II. FORMALISM

We plot the Feynman diagrams of the decay process $J/\psi \to K^-K^+a_1(1260)$ involving a triangle loop in Fig. 1, where the meson J/ψ first decays into two vector mesons ϕ, K^* and a pesudoscalar meson $\bar{K}$, and then the meson ϕ is converted into K and $\bar{K}$. The $\bar{K}$ can move faster than K^*, so they can combine to generate the $a_1(1260)$. Finally, we consider that the $a_1(1260)$ continues to decay into $\pi^+\rho^-$ final states.

We take Fig. 1(b) for example to perform the following discussion since Fig. 1(a) and (b) have nearly the same amplitude. In order to find the position of triangle singularity in complex-q plane, analogously to Ref. [9,21,51], we use

$$q_+^{\rm on} = q_-^{\rm a}, \quad \text{and} \quad q_+^{\rm on} = \frac{\lambda^{\frac{1}{2}}(s, M_\phi^2, M_{K^{*+}}^2)}{2\sqrt{s}}, \tag{1}$$

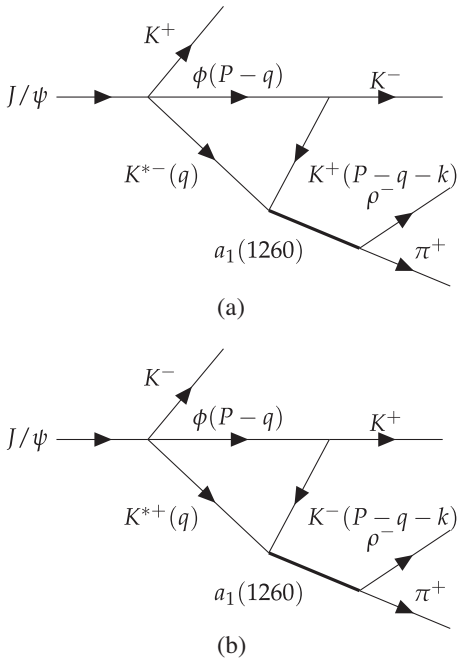

FIG. 1. The Feynman diagrams of the decay process $J/\psi \to K^-K^+a_1(1260), a_1 \to \pi^+\rho^-$ involving a triangle loop.

where the $q_+^{\rm on}$ is the on-shell three-momentum of the K^{*+} in the center of mass frame of ϕK^{*+}, s denotes the squared invariant mass of ϕ and K^{*+}, and $\lambda(x,y,z) = x^2 + y^2 + z^2 - 2xy - 2yz - 2xz$ is the Kählen function.

Meanwhile, $q_-^{\rm a}$ can be obtained by analyzing the singularity structure of the triangle loop, which is given by

$$q_-^{\rm a} = \gamma(\nu E_{K^{*+}} - p^*_{K^{*+}}) - i\epsilon \tag{2}$$

with definition

$$\nu = \frac{k}{E_{a_1}}, \qquad \gamma = \frac{1}{\sqrt{1-\nu^2}} = \frac{E_{a_1}}{m_{a_1}},$$
$$E_{K^{*+}} = \frac{m_{a_1}^2 + m_{K^{*+}}^2 - m_{k^-}^2}{2m_{a_1}}, \qquad p^*_{K^{*+}} = \frac{\lambda^{\frac{1}{2}}(m_{a_1}^2, M_{K^-}^2, M_{K^{*+}}^2)}{2m_{a_1}}, \tag{3}$$

where $E_{K^{*+}}$ and $p^*_{K^{*+}}$ are the energy and momentum of the K^{*+} meson in the center of mass frame of the $K^{*+}\phi$ system, ν and γ are the velocity of the a_1 and Lorentz boost factor, respectively. In addition,

$$E_{a_1} = \frac{s + m_{a_1}^2 - m_{K^-}^2}{2\sqrt{s}}, \qquad k = \frac{\lambda^{\frac{1}{2}}(s, m_{a_1}^2, m_{K^-}^2)}{2\sqrt{s}}. \tag{4}$$

When Eq. (1) is established we need to consider the case that all three intermediate particles in the triangle loop are on shell and the angular z between momentum q and k is taken as $z = -1$, i.e., the momentum of particle K^{*+} is

antiparallel to the momentum of the $a_1(1260)$ in the $K^{*+}K^-$ center of mass frame. Now, by letting the mass of the $a_1(1260)$ be slightly larger than the mass sum of K^* and K mesons and applying Eq. (1), one can find a triangle singularity at around $\sqrt{s} = 1920$ MeV keeping $K^{*+} = 891.66$ MeV and $K^- = 493.68$ MeV [52] in mind. If we use in Eq. (1) complex masses $(M - i\Gamma/2)$ of vector mesons which include widths of K^* and ϕ mesons, the solution of Eq. (1) is then $(1920 - 48i)$ MeV. This solution implies that the triangle singularity has a width of 96 MeV.

A. The decay process $J/\psi \to K^-\phi K^{*+}$

Before writing the whole amplitude of the Feynman diagram in Fig. 1(b), the generalized vertex $V_{J/\psi,K^-\phi K^{*+}}$ needs to be calculated first. Experimentally we have the $K^*\phi$ invariant mass distribution in Fig. 10(a) of Ref. [53]. One can find a broad peak around 1800 MeV in $K^*\phi$ invariant mass distribution. This structure indicates that there should be a better form factor in the one to three amplitude range, which comes from the interaction of $K^*\phi$ to give a resonance of around 1800 MeV. This structure is somewhat important since if we do not add this structure in the one to three vertex, after carefully calculation one can not find a clear singularity in $K^+a_1(1260)$ invariant mass distribution of $J/\psi \to K^-K^+a_1(1260)$ decay process. In that case, the clear peak of $K^+a_1(1260)$ in $|t_T|^2$ will be expunged by the phase space and kinematic factors in the total $J/\psi \to K^-K^+a_1(1260)$ decay process.

Now we introduce some kind of propagator X that can decay into $K^*\phi$. The process then becomes $J/\psi \to K^-X \to K^-\phi K^{*+}$. Under conservation of strangeness, isospin, and spin for $X \to K^*\phi$, the low-lying vector meson X should satisfy strangness $= 0$, isospin $= 1/2$, and spin $= 1$. In Refs. [54,55], the vector meson $K_1(1650)$ is well regarded as dynamically-generated state from the vector-vector interaction which corresponds to the pole position (1665,−95). It is supposed to couple with two vector mesons such as $K^*\rho, K^*\omega, K^*\phi$. However, the width of $K_1(1650)$ is not very large and the mass of $K_1(1650)$ is somewhat far away from the $K^*\phi$ threshold which results in a small possibility of decay from $K_1(1650)$ to $K^*\phi$ final states. Alternatively, a pole position (1823,−61) was reported by applying a different subtraction constants, $a = -3.1$ [55]. This potential K_1 state has a suitable width and its mass 1823 MeV is close to the $K^*\phi$ threshold. Also, its coupling from $K^*\phi$ shown in Ref. [55] is relatively large. On basis of the above considerations, we choose this reported pole of K_1 type as the propagator X, which has a resonant shape

$$F(M_{K^*\phi}) = \frac{M_X\Gamma_{M_X}}{M^2_{K^*\phi} - M^2_X + iM_X\Gamma_{M_X}}, \tag{5}$$

where M_X, Γ_{M_X} are taken by 1823 MeV and 122 MeV, respectively. The $J/\psi \to K^-\phi K^{*+}$ decay amplitude can then be written as

$$-it_{J/\psi,K^-\phi K^{*+}} = -i\mathcal{C}\varepsilon_{ijk}\epsilon_i(J/\psi)\epsilon_j(\phi)\epsilon_k(K^*)F(M_{K^{*+}\phi}). \tag{6}$$

The coefficient $\mathcal{C}$ is obtained by comparing the calculated $J/\psi \to \phi K^-K^{*+}$ decay branching ratio with those from the experiment. Note that the amplitude in Eq. (6) is a bit rough, since we have neglected all the other contributions to the process, such as resonances that couple to each pair of the three final-state mesons. In Refs. [53,56] the decay branching ratio for $J/\psi \to \phi K^*\bar{K} + \text{c.c.}$ is $(2.18 \pm 0.23) \times 10^{-3}$. Here, we only focus on the $J/\psi \to \phi K^-K^{*+}$ process and the relation between above the two-decay branching ratio is

$$\text{Br}(J/\psi \to \phi K^-K^{*+}) = \frac{1}{4}\text{Br}(J/\psi \to \phi K^*\bar{K} + \text{c.c.}). \tag{7}$$

The differential decay width over the invariant mass distribution $K^{*+}\phi$ can be written as

$$\frac{d\Gamma_{J/\psi\to\phi K^-K^{*+}}}{dM_{\text{inv}}(K^{*+}\phi)} = \frac{1}{(2\pi)^5}\frac{|\vec{k}^*_{K^{*+}}||\vec{k}_{K^-}|}{16m_J^2} \cdot \overline{\sum}|t_{J/\psi\to\phi K^-K^{*+}}|^2 d\Omega^*_{K^{*+}}d\Omega_{K^-}, \tag{8}$$

where m_J is the mass of J/ψ, $|\vec{k}^*_{K^{*+}}|$ and $\Omega^*_{K^{*+}}$ are the absolute value of the K^{*+} three-momentum and the K^{*+} solid angle in the center of mass frame of the final $K^{*+}\phi$ system, respectively. Whereas, $|\vec{k}_{K^-}|$ and $\Omega_{k_{K^-}}$ are the absolute value of the K^- three-momentum and the K^- solid angle in the rest frame of the initial J/ψ meson, respectively. To perform the calculation in Eq. (8), we use the polarization summation formula

$$\sum_{\text{pol}}\varepsilon_\mu(p)\varepsilon_\nu(p) = -g_{\mu\nu} + \frac{p_\mu p_\nu}{m^2}. \tag{9}$$

Then one can obtain

$$\frac{\mathcal{C}^2}{\Gamma_{J/\psi}} = \frac{\text{Br}(J/\psi \to \phi K^-K^{*+})}{\int dM_{\text{inv}}(K^{*+}\phi)\frac{d\Gamma_{J/\psi\to\phi K^-K^{*+}}}{dM_{\text{inv}}(K^{*+}\phi)}}. \tag{10}$$

B. The role of triangle mechanism in the decay $J/\psi \to K^-K^+a_1(1260), a_1 \to \pi^+\rho^-$

In the previous subsection we calculated the transition strength of the decay process $J/\psi \to K^-\phi K^{*+}$. Now we focus on the triangle diagram amplitudes required by $J/\psi \to K^-K^+a_1(1260)$, $a_1 \to \pi^+\rho^-$ process. The Feynman diagrams are shown in Fig. 1 where J/ψ decays into $\phi K^*\bar{K}$, the ϕ decays into $\bar{K}K$, and then the K^* and $\bar{K}$ fuse into the $a_1(1260)$. The particles' identification and momentum information are labeled in the diagrams. This triangle mechanism can take place as long as the $a_1(1260)$ couples

to the $K^*\bar{K}$ pair, thus the triangle singularity induced decay process can be used to gain valuable information for the $a_1(1260)$. Finally, the $a_1(1260)$ decays into $\pi^+\rho^-$. At the beginning, we need to evaluate the ϕK^+K^- vertex for Fig. 1(b) which can be obtained from the vector-pseudoscalar Lagrangian

$$\mathcal{L}_{VPP} = -ig\langle V^\mu[P, \partial_\mu P]\rangle, \tag{11}$$

where the $\langle\rangle$ represents the $SU(3)$ trace. The coupling constant g, vector meson mass, and the decay constant of the pion are taken as [57]

$$g = \frac{M_V}{2f_\pi}, \qquad M_V = 800 \text{ MeV}, \qquad f_\pi = 93 \text{ MeV}. \tag{12}$$

The V and P in Eq. (11) are the vector-meson matrix and pseudoscalar-meson matrix in the $SU(3)$ group, respectively [58]

$$P = \begin{pmatrix} \frac{\pi^0}{\sqrt{2}} + \frac{\eta}{\sqrt{3}} + \frac{\eta'}{\sqrt{6}} & \pi^+ & K^+ \\ \pi^- & -\frac{\pi^0}{\sqrt{2}} + \frac{\eta}{\sqrt{3}} + \frac{\eta'}{\sqrt{6}} & K^0 \\ K^- & \bar{K}^0 & -\frac{\eta}{\sqrt{3}} + \sqrt{\frac{2}{3}}\eta' \end{pmatrix},$$
$$V = \begin{pmatrix} \frac{\rho^0}{\sqrt{2}} + \frac{\omega}{\sqrt{2}} & \rho^+ & K^{*+} \\ \rho^- & -\frac{\rho^0}{\sqrt{2}} + \frac{\omega}{\sqrt{2}} & K^{*0} \\ K^{*-} & \bar{K}^{*0} & \phi \end{pmatrix}. \tag{13}$$

The total amplitude of the $J/\psi \to K^-K^+a_1$ decay process as shown in Fig. 1(b) can be written down directly

$$\begin{aligned} -it = &-i\mathcal{C}F(K^-a_1)\varepsilon_{ijk}\varepsilon_i(J/\psi)\varepsilon_j(\phi)\varepsilon_k(K^*) \\ &\cdot \int \frac{d^4q}{(2\pi)^4} \frac{i}{q^2 - m^2_{K^{*+}} + im_{K^*}\Gamma_{K^*}} \\ &\cdot \frac{i}{(P-q)^2 - m^2_\phi + im_\phi\Gamma_\phi} \frac{i}{(P-q-k)^2 - m^2_{K^-} + i\varepsilon} \\ &\cdot (-ig)(p_{K^+} - p_{K^-})_\mu \varepsilon^\mu(\phi)(-ig_{a_1,K^{*+}K^-})\varepsilon(K^*)\cdot\varepsilon(a_1), \end{aligned} \tag{14}$$

where the $g_{a_1,K^{*+}K^-}$ is the coupling of the $a_1(1260)$ to $K^{*+}K^-$, and $P^0 = M_{\text{inv}}(K^+a_1)$ in the K^+a_1 rest frame. We have assumed that only the spatial components of the polarization vector of vector mesons are nonvanishing, which leads to the vanishing zero component of the polarization vector and the completeness relation for the polarization vectors written as

$$\sum_{\text{pol}} \varepsilon_\mu(p)\varepsilon_\nu(p) = \delta_{\mu\nu} + \frac{p_\mu p_\nu}{m^2}, \tag{15}$$

where i, j are Lorentz indices from 1 to 3. In Eq. (14), after integrating over $\vec{q}$ only the vector $\vec{k}$ remains, therefore, for a function $f(\vec{q}, \vec{k})$ we have

$$\int d^3\vec{q}\, q_i f(\vec{q}, \vec{k}) = Ak_i,$$
$$A = \int d^3\vec{q} \frac{\vec{q}\cdot\vec{k}}{|\vec{k}|^2} f(\vec{q}, \vec{k}). \tag{16}$$

Considering Eqs. (15) and (16), Eq. (14) can be simplified as

$$\begin{aligned} t = &\mathcal{C}F\varepsilon_{ijk}\varepsilon_i(J/\psi)\varepsilon_k(a_1) i \int \frac{d^4q}{(2\pi)^4} \frac{1}{q^2 - m^2_{K^{*+}} + im_{K^*}\Gamma_{K^*}} \\ &\times \frac{(2k+q)_j g\, g_{a_1,K^{*+}K^-}}{(P-q)^2 - m^2_\phi + im_\phi\Gamma_\phi} \frac{1}{(P-q-k)^2 - m^2_{K^-} + i\varepsilon} \\ = &\, i\mathcal{C}F(M_{\text{inv}}(K^+a_1))g g_{a_1,K^{*+}K^-}\varepsilon_{ijk}\varepsilon_i(J/\psi)\varepsilon_k(a_1)k_j t_T. \end{aligned} \tag{17}$$

where the zero component of q integration in Eq. (17) has been performed analytically by residue theory, leads to a three-dimensional loop intergral t_T which can be integrated numerically

$$\begin{aligned} t_T = &\int \frac{\mathrm{d}^3q}{(2\pi)^3} \frac{1}{8\omega_{K^-}\omega_\phi\omega_{K^{*+}}} \frac{1}{k^0 - \omega_{K^-} - \omega_\phi} \\ &\times \frac{1}{M_{\text{inv}}(K^+a_1) + \omega_{K^{*+}} + \omega_{K^-} - k^0} \\ &\times \frac{1}{M_{\text{inv}}(K^+a_1) - \omega_{K^{*+}} - \omega_{K^-} - k^0 + i\frac{\Gamma_{K^{*+}}}{2}} \\ &\times \left[\frac{2M_{\text{inv}}(K^+a_1)\omega_{K^{*+}} + 2k^0\omega_{K^-}}{M_{\text{inv}}(K^+a_1) - \omega_\phi - \omega_{K^{*+}} + i\frac{\Gamma_\phi}{2} + i\frac{\Gamma_{K^{*+}}}{2}} \right. \\ &\left. - \frac{2(\omega_{K^{*+}} + \omega_{K^-})(\omega_{K^{*+}} + \omega_\phi + \omega_{K^-})}{M_{\text{inv}}(K^+a_1) - \omega_\phi - \omega_{K^{*+}} + i\frac{\Gamma_\phi}{2} + i\frac{\Gamma_{K^{*+}}}{2}} \right] \\ &\times \left(2 + \frac{\vec{q}\cdot\vec{k}}{\vec{k}^2}\right), \end{aligned} \tag{18}$$

with

$$\omega_\phi = \sqrt{\vec{q}^2 + m^2_\phi}, \qquad \omega_{K^-} = \sqrt{(\vec{q}+\vec{k})^2 + m^2_{K^-}},$$
$$\omega_{K^{*+}} = \sqrt{\vec{q}^2 + m^2_{K^{*+}}}, \qquad k^0 = \frac{M^2_{\text{inv}}(K^+a_1) + m^2_{K^+} - m^2_{a_1}}{2M_{\text{inv}}(K^+a_1)},$$
$$|\vec{k}| = \frac{\lambda^{1/2}(M^2_{\text{inv}}(K^+a_1), m^2_{K^+}, m^2_{a_1})}{2M_{\text{inv}}(K^+a_1)}. \tag{19}$$

The width of vector mesons K^{*+} and ϕ are taken as $\Gamma_{K^{*+}} = 48$ MeV and $\Gamma_\phi = 4.25$ MeV, respectively.

The above integral is regularized with a cutoff $q_{\max}$ on the loop integral $|\vec{q}|$. We take $q_{\max} = 950$ as in [59] to produce $a_1(1260)$ in the chiral unitary approach. In the $|\vec{t}|^2$ level we need to sum over the spin structure of the external vector mesons. Applying Eq. (9) we have

$$\overline{\sum_{\text{pol}}}\varepsilon_{ijk}\varepsilon_i(J/\psi)\varepsilon_k(a_1)k_j\varepsilon_{\mu\nu\rho}\varepsilon_\mu(J/\psi)\varepsilon_\rho(a_1)k_\nu = \frac{1}{3}\left(\frac{2\vec{p}^2\vec{k}^2}{m_{a_1}^2} - \frac{2(\vec{p}\cdot\vec{k})^2}{m_{a_1}^2} + 6\vec{k}^2\right), \tag{20}$$

where $\vec{p} = \vec{P} - \vec{k}$ is the three-vector of the final $a_1(1260)$ meson, and the mass of the $a_1(1260)$ is taken as 1230 MeV from particle data group [52]. Then the distribution of invariant mass $M_{\text{inv}}(K^+a_1)$ in the decay $J/\psi \to K^-K^+a_1(1260)$ can be written as

$$\frac{1}{\Gamma_{J/\psi}}\frac{d\Gamma_{J/\psi\to K^-K^+a_1(1260)}}{dM_{\text{inv}}(K^+a_1)} = \frac{1}{(2\pi)^3}\frac{|\vec{\tilde{q}}_{K^+}||\vec{p}_{K^-}|}{4M^2}\overline{\sum}|t|^2, \tag{21}$$

where M is the mass of the J/ψ meson. The three-momenta $|\vec{\tilde{q}}_{K^+}|$ and $|\vec{p}_{K^-}|$ in Eq. (26) are given by

$$|\vec{\tilde{q}}_{K^+}| = \frac{\lambda^{1/2}(M_{\text{inv}}^2(K^+a_1), m_{K^+}^2, m_{a_1}^2)}{2M_{\text{inv}}(K^+a_1)},$$
$$|\vec{p}_{K^-}| = \frac{\lambda^{1/2}(M^2, m_{K^-}^2, M_{\text{inv}}^2(K^+a_1))}{2M}. \tag{22}$$

Then the differential branching ratio of the decay process $J/\psi \to K^-K^+a_1(1260)$ can be written as

$$\frac{1}{\Gamma_{J/\psi}}\frac{d\Gamma_{J/\psi\to K^-K^+a_1(1260)}}{dM_{\text{inv}}(K^+a_1)} = \frac{1}{(2\pi)^3}\frac{|\vec{\tilde{q}}_{K^+}||\vec{p}_{K^-}|}{4M^2}\frac{\mathcal{C}^2}{\Gamma_{J/\psi}}F^2(M_{\text{inv}}(K^+a_1))g^2g_{a_1,K^{*+}K^-}^2 \times\frac{1}{3}\left(\frac{2\vec{p}^2\vec{k}^2}{m_{a_1}^2} - \frac{2(\vec{p}\cdot\vec{k})^2}{m_{a_1}^2} + 6\vec{k}^2\right)\Big|t_T|^2, \tag{23}$$

where the $a_1(1260) \to K^*\bar{K}$ vertex is obtained from the chiral unitary approach of Ref. [45] with $g_{a_1,K^*K} = 2390$ MeV. Furthermore, to perform the numerical calculations, we choose the z-axis along the direction of the vector k without loss of generality.

Now we add the final $a_1(1260) \to \pi^+\rho^-$ decay process to our total amplitude. To calculate the $|t|^2$, we need to sum over the spin structure of the external vector mesons. Applying Eq. (9) we have

$$\overline{\sum_{\text{pol}}}\varepsilon_{ijk}\varepsilon_i(J/\psi)\varepsilon_k(\rho)k_j\varepsilon_{\mu\nu\rho}\varepsilon_\mu(J/\psi)\varepsilon_\rho(\rho)k_\nu = \frac{1}{3}\left(\frac{2\vec{p}'^2\vec{k}^2}{m_\rho^2} - \frac{2(\vec{p}'\cdot\vec{k})^2}{m_\rho^2} + 6\vec{k}^2\right), \tag{24}$$

where $\vec{p}'$ denotes the three-momentum of the final ρ meson, and $m_\rho = 782$ MeV denotes the mass of the ρ meson. Then we have

$$\overline{\sum_{\text{pol}}}|t|^2 = \mathcal{C}^2F^2(M_{\text{inv}}(K^+a_1))g^2g_{a_1,\pi^+\rho^-}^2 \times\frac{1}{3}\left(\frac{2\vec{p}'^2\vec{k}^2}{m_\rho^2} - \frac{2(\vec{p}'\cdot\vec{k})^2}{m_\rho^2} + 6\vec{k}^2\right)|t_T|^2. \tag{25}$$

After applying the calculation details in [27], one can reach the double differential mass distribution in $M_{\text{inv}}(K^+a_1)$ and $M_{\text{inv}}(\pi^+\rho^-)$

$$\frac{1}{\Gamma_{J/\psi}}\frac{d^2\Gamma_{J/\psi\to K^-K^+a_1(1260),a_1\to\pi^+\rho^-}}{dM_{\text{inv}}(K^+a_1)dM_{\text{inv}}(\pi^+\rho^-)} = \frac{1}{4\pi}\frac{1}{(2\pi)^5}\frac{|\vec{p}_{K^-}||\vec{k}|}{4M^2}\frac{\mathcal{C}^2}{\Gamma_{J/\psi}}|F(M_{\text{inv}}(K^+a_1))|^2g^2|t_T|^2|\vec{\tilde{q}}_\rho| \times\frac{1}{3}\left(\frac{2\vec{p}'^2\vec{k}^2}{m_\rho^2} - \frac{2(\vec{p}'\cdot\vec{k})^2}{m_\rho^2} + 6\vec{k}^2\right)\cdot|t_{K^{*+}K^-\to\pi^+\rho^-}|^2d\Omega_k, \tag{26}$$

where the coupling $g_{a_1,\pi^+\rho^-}$ has been absorbed into $t_{K^{*+}K^-\to\pi^+\rho^-}$ denoting the isospin-one amplitude of the final $VP \to VP$ scattering. This amplitude can be calculated by solving the Bethe-Salpeter equation

$$t = \frac{V}{1 - VG}, \tag{27}$$

where G is the loop function given in [45], and V is a 2×2 matrix of the interaction kernel, the two channels are taken by 1 for K^*K and 2 for $\rho\pi$. The corresponding transition potentials come from the Lagrangian involving $VVPP$ coupling under the local hidden-gauge approach [45]

$$V_{ij} = -\frac{C_{ij}}{8f^2}\Big[3s - (M^2 + m^2 + M'^2 + m'^2) - \frac{1}{s}(M^2 - m^2)(M'^2 - m'^2)\Big], \tag{28}$$

where the C_{ij} are coefficients related to different particles and isospin basis (S, I) [45]. M and m are respectively vector and pseudoscalar mesons in channel i, and M' and m' are respectively vector and pseudoscalar mesons in channel j. Also, after calculating the corresponding $C-G$ coefficient we have

$$t_{K^{*+}K^-\to\pi^+\rho^-} = -\frac{1}{2} t_{K^*\bar{K}\to\pi\rho}. \tag{29}$$

The three-momenta $|\vec{\tilde{q}}_\rho|$ and $|\vec{p}_{K^-}|$ in Eq. (26) are given by

$$|\vec{\tilde{q}}_\rho| = \frac{\lambda^{1/2}(M^2_{\rm inv}(\pi^+\rho^-), m^2_\pi, m^2_\rho}{2M_{\rm inv}(\pi^+\rho^-)},$$
$$|\vec{p}_{K^-}| = \frac{\lambda^{1/2}(M^2, m^2_{K^-}, M^2_{\rm inv}(K^+a_1))}{2M}. \tag{30}$$

In addition, without loss of generality, we choose the four vector p' of the final ρ^- meson as the z-axis, then there exists a solid angle integral element $\frac{1}{4\pi} d\Omega_k$ in Eq. (26) according to the general three-body phase space integration formalism [52]. Finally, the integration range of $M_{\rm inv}(\pi^+\rho^-)$ is $(m_{\pi^+} + m_{\rho^-}, M_{\rm inv}(K^+a_1) - m_{K^-})$ as usual and there is also a factor of four added in to the numerical calculation due to the two Feynman diagram contributions for the underlying process.

III. NUMERICAL CALCULATION

At the beginning, we present in Figs. 2(a)–2(c) the absolute value, the square of the absolute value, the imaginary part, and the real part of the triangle loop amplitude t_T in Eq. (18) as functions of the K^+a_1 invariant mass, where the invariant masses of final $\pi^+\rho^-$ states are taken as 1300, 1350, and 1400 MeV, respectively. We focus on Fig. 2(c) obtained by taking the invariant masses of $\pi^+\rho^-$ a little larger than the K^-K^{*+} threshold (1385 MeV) first. Note that in this case the smallest value of $M_{\rm inv}(K^-a_1)$ is about 1900 MeV (nearby the K^+a_1 threshold). From this diagram we can see that there is a peak in $|t_T|^2$ located at around 1920 MeV with a width of 100 MeV. This width mainly originates from the width of the vector propagators K^* and ϕ, which is basically consistent with the prediction of 96 MeV. It is also found from Figs. 2(a)–2(c) that as the chosen mass of $a_1(1260)$ becomes larger, the width of the peak in $|t_T|^2$ becomes larger. A bump in $\mathrm{Im}(t_T)$ can be found nearby 1920 MeV related with the triangle singularity, which has been addressed in Refs. [26,31]. After comparing with Figs. 2(a) and 2(b), we find that the

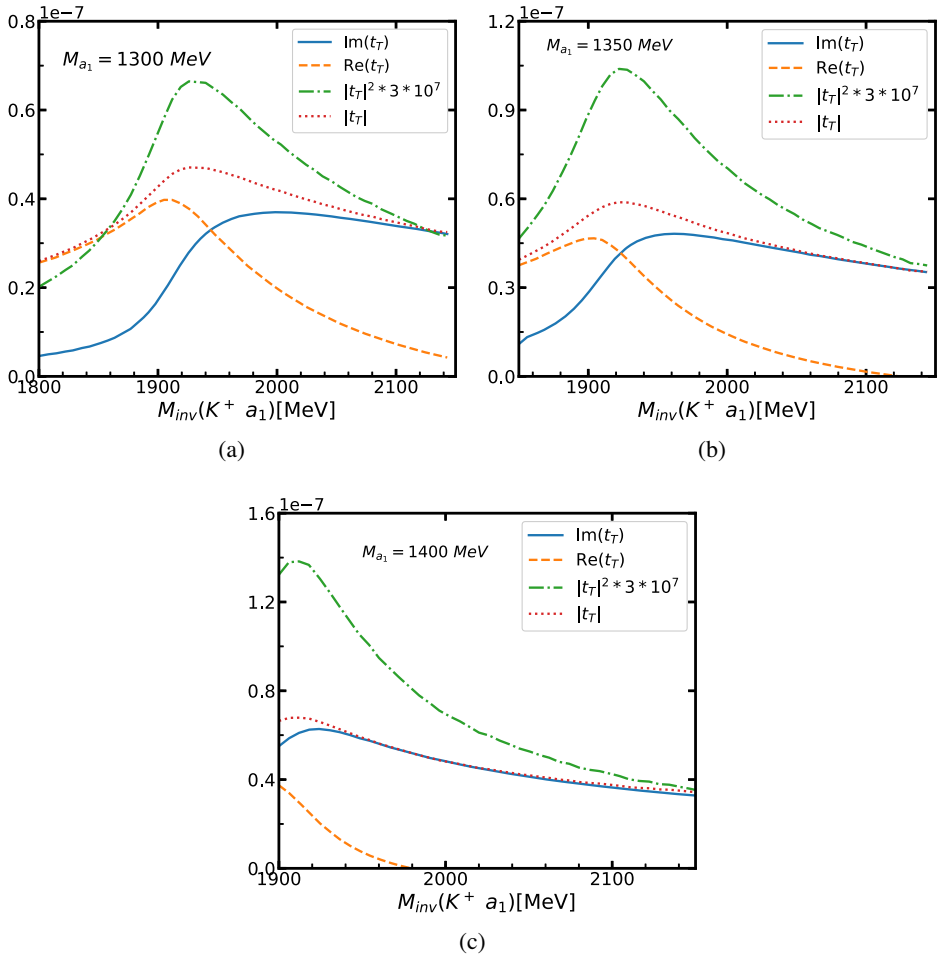

FIG. 2. Triangle amplitude t_T as a function of $M_{\rm inv}(K^+a_1)$ for (a) $M_{\rm inv}(\pi^+\rho^-) = 1300$ MeV, (b) $M_{\rm inv}(\pi^+\rho^-) = 1350$ MeV, and (c) $M_{\rm inv}(\pi^+\rho^-) = 1400$ MeV. $|t_T|^2, |t_T|, \mathrm{Re}(t_T)$ and $\mathrm{Im}(t_T)$ are plotted using the green, red, yellow, and blue curves, respectively.

strengths of the absolute value, the square of the absolute value, the imaginary part, and the real part of the triangle loop amplitude t_T become smaller as the M_{a_1} gets smaller. This suggests all these quantities can obtain sizeable enhancement when M_{a_1} is close to the K^-K^{*+} threshold. Also, the position of the peak in $|t_T|^2$ leaves basically unchanged due to the triangle mechanism. We observe a broad peak in $\mathrm{Re}(t_T)$ nearby the $K^*\phi$ threshold which has been suggested and discussed in Refs. [26,31]. Moreover, the primary bump in Fig. 2(c) has converted into broad bumps in Figs. 2(a) and 2(b) on account of the potential deviation from the K^-K^{*+} threshold required by the triangle mechanism.

As shown in Fig. 3, we plot the differential branching ratio of the underlying decay process $\frac{1}{\Gamma}\frac{d^2\Gamma}{dM_{\rm inv}(K^+a_1)dM_{\rm inv}(\pi^+\rho^-)}$, defined in Eq. (26), where the $M_{\rm inv}(\pi^+\rho^-)$ has been integrated from $(m_{\pi^+}+m_{\rho^-})$ to $(M_{\rm inv}(K^+a_1)-m_{K^-})$. There is a clear peak around 1920 MeV as predicted by the triangle mechanism. The strength of the differential branching ratio can reach 2.4×10^{-8} MeV^{-2}. Additionally, the upper part of the invariant mass distribution drops more slowly than the lower part because of the polarized factor in Eq. (9), which produces large contribution when $M_{\rm inv}(\pi^+\rho^-)$ is large. We also plot the triangle amplitude $|t_T|$ in Eq. (18) as a function of $M_{\rm inv}(\pi^+\rho^-)$ with $M_{\rm inv}(K^+a_1)$ taken by 1920, 1940, and 1960 MeV in Fig. 4, respectively. There is a peak near 1390 MeV in all of these three cases which is the direct reflection of the triangle mechanism; to obtain the triangle singularities, one should let the $M_{\rm inv}(\pi^+\rho^-)$ slightly larger than the K^-K^{*+} threshold. It is desirable to mention that there is a very small reduction on the position of the peak as the $M_{\rm inv}(K^+a_1)$ increases from 1920 MeV to 1960 MeV. On the other hand, the distribution with the $M_{\rm inv}(K^+a_1)$ taken as 1920 MeV has the largest strength which is enhanced by the triangle mechanism. As the $M_{\rm inv}(K^+a_1)$ increases from the position of triangle singularity, the strength becomes lower and the width of the peak gets larger.

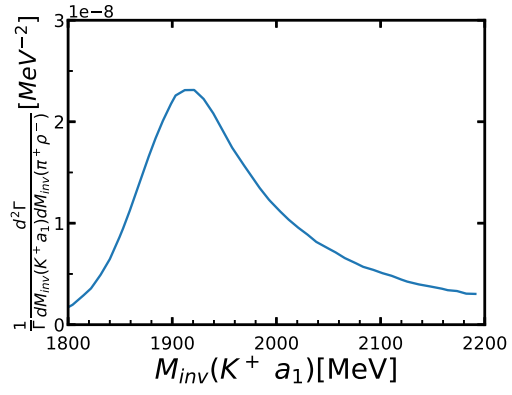

FIG. 3. The differential branching ratio $\frac{1}{\Gamma}\frac{d^2\Gamma}{dM_{\rm inv}(K^+a_1)dM_{\rm inv}(\rho\pi)}$ described as in Eq. (26) as a function of $M_{\rm inv}(K^+a_1)$. The integration range of $M_{\rm inv}(\pi^+\rho^-)$ is given by the text.

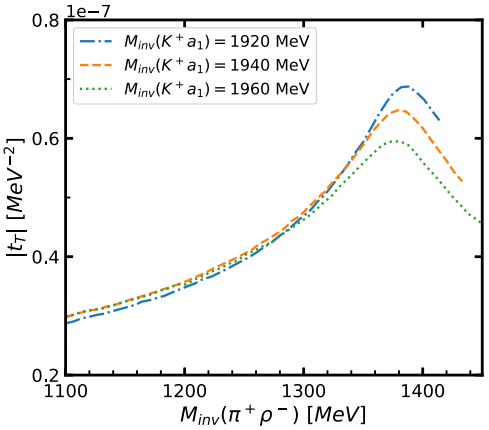

FIG. 4. Triangle amplitude $|t_T|$ as a function of $M_{\rm inv}(\pi^+\rho^-)$ for $M_{\rm inv}(K^+a_1)=1920$, 1940, and 1960 MeV.

Next, we show in Fig. 5 the differential branching ratio $\frac{1}{\Gamma}\frac{d\Gamma}{dM_{\rm inv}(\pi^+\rho^-)}$, described as in Eq. (26) as a function of $M_{\rm inv}(\pi^+\rho^-)$ for $M_{\rm inv}(K^+a_1)=1920$, 1940, and 1960 MeV. We find that the $M_{\rm inv}(\pi^+\rho^-)$ distribution around 1920 MeV has the largest strength over the three cases, which is a natural result of the triangle mechanism. Note that the position of the peak in the three cases increases as the $M_{\rm inv}(\pi^+\rho^-)$ increases. The peaks of all three distributions deviate from the K^-K^{*+} threshold due to the contribution coming from the polarized factor involving k^2 in Eq. (9).

Finally, we integrate out two invariant masses in Eq. (26) in order to obtain the branching ratio of the total decay process $J/\psi\to K^-K^+a_1(1260)$. The integration range of $M_{\rm inv}(K^+a_1)$ is $(m_{K^+}+m_{a_1}, m_{J/\psi}-m_{K^+}-m_{a_1})$, while those for $M_{\rm inv}(\pi^+\rho^-)$ is $(m_{\rho^-}+m_{\pi^+}, M_{\rm inv}(K^+a_1)-m_{K^-})$. We find

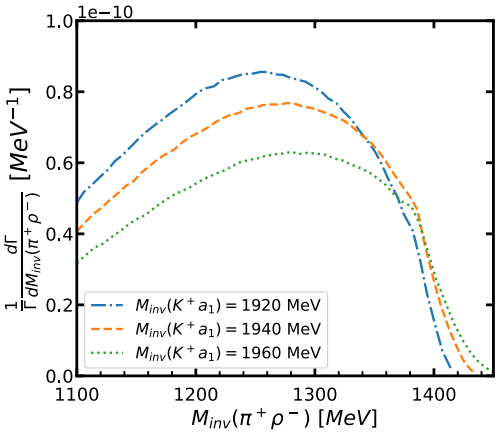

FIG. 5. The differential branching ratio $\frac{1}{\Gamma}\frac{d^2\Gamma}{dM_{\rm inv}(K^+a_1)dM_{\rm inv}(\pi^+\rho^-)}$ described as in Eq. (26) as a function of $M_{\rm inv}(\pi^+\rho^-)$ for $M_{\rm inv}(K^+a_1)=1920$, 1940, and 1960 MeV.

$$\mathrm{Br}(J/\psi \to K^- K^+ a_1(1260), a_1 \to \pi^+ \rho^-) = 4.033 \times 10^{-6}, \tag{31}$$

and then one can easily obtain

$$\mathrm{Br}(J/\psi \to K^- K^+ a_1(1260), a_1 \to \pi\rho) = 1.210 \times 10^{-5}. \tag{32}$$

In addition, we obtain the decay branching ratio of $J/\psi \to K^- K^+ a_1(1260)$ by using Eq. (23)

$$\mathrm{Br}(J/\psi \to K^- K^+ a_1(1260)) = 3.501 \times 10^{-5}. \tag{33}$$

These rates are accessible at BESIII within the observation capability.

IV. CONCLUSION

The present study was designed to determine the effect of the triangle mechanism of the decay process of $J/\psi \to K^- K^+ a_1(1260)$. The results of this investigation show that there is a triangle singularity around 1920 MeV for the invariant mass $M_{\mathrm{inv}}(K^+ a_1)$. The strength of the differential branching ratio $\frac{1}{\Gamma}\frac{d^2\Gamma}{dM_{\mathrm{inv}}(K^+ a_1) dM_{\mathrm{inv}}(\rho^- \pi^+)}$, reaches 2.4×10^{-8} MeV^{-1}. We have applied the experimental data of the branching ratio of the decay $J/\psi \to \bar{K} K^* \phi$ to determine the coupling strength of the $J/\psi \bar{K} K^* \phi$ vertex. We also evaluate the triangle amplitude $|t_T|$ and the differential branching ratio $\frac{1}{\Gamma}\frac{d^2\Gamma}{dM_{\mathrm{inv}}(K^+ a_1) dM_{\mathrm{inv}}(\rho^- \pi^+)}$ as functions of $M_{\mathrm{inv}}(\pi^+ \rho^-)$. There are deviations of all three distributions in the latter from the $K^- K^{*+}$ threshold on account of the contribution coming from the polarized factor involving k^2. We hope that the future the LHCb, Belle-II, and BESIII experimental data will focus on the $J/\psi \to K^- K^+ a_1(1260)$ process and clarify the role played by the triangle singularities in this decay process, which can provide valuable information for the low-lying axial-vector mesons $a_1(1260)$.

ACKNOWLEDGMENTS

The authors thank professor Jujun Xie for his patient guidance. Hao Sun is supported by the National Natural Science Foundation of China (Grant No. 12075043).

[1] R. Karplus, C. M. Sommerfield, and E. H. Wichmann, Phys. Rev. **111**, 1187 (1958).
[2] L. Landau, Nucl. Phys. **13**, 181 (1959).
[3] R. F. Peierls, Phys. Rev. Lett. **6**, 641 (1961).
[4] I. J. R. Aitchison, Phys. Rev. **133**, B1257 (1964).
[5] J. B. Bronzan, Phys. Rev. **134**, B687 (1964).
[6] S. Coleman and R. E. Norton, Nuovo Cimento **38**, 438 (1965).
[7] C. Schmid, Phys. Rev. **154**, 1363 (1967).
[8] F.-K. Guo, X.-H. Liu, and S. Sakai, Prog. Part. Nucl. Phys. **112**, 103757 (2020).
[9] M. Bayar, F. Aceti, F.-K. Guo, and E. Oset, Phys. Rev. D **94**, 074039 (2016).
[10] C. Adolph *et al.* (COMPASS Collaboration), Phys. Rev. Lett. **115**, 082001 (2015).
[11] X.-H. Liu, M. Oka, and Q. Zhao, Phys. Lett. B **753**, 297 (2016).
[12] M. Mikhasenko, B. Ketzer, and A. Sarantsev, Phys. Rev. D **91**, 094015 (2015).
[13] F. Aceti, L. R. Dai, and E. Oset, Phys. Rev. D **94**, 096015 (2016).
[14] M. Ablikim *et al.* (BESIII Collaboration), Phys. Rev. Lett. **108**, 182001 (2012).
[15] J.-J. Wu, X.-H. Liu, Q. Zhao, and B.-S. Zou, Phys. Rev. Lett. **108**, 081803 (2012).
[16] F. Aceti, W. H. Liang, E. Oset, J. J. Wu, and B. S. Zou, Phys. Rev. D **86**, 114007 (2012).
[17] X.-G. Wu, J.-J. Wu, Q. Zhao, and B.-S. Zou, Phys. Rev. D **87**, 014023 (2013).
[18] N. N. Achasov, A. A. Kozhevnikov, and G. N. Shestakov, Phys. Rev. D **92**, 036003 (2015).
[19] N. N. Achasov and G. N. Shestakov, Pis'ma Zh. Eksp. Teor. Fiz. **107**, 292 (2018) [JETP Lett. **107**, 276 (2018)].
[20] K. Moriya *et al.* (CLAS Collaboration), Phys. Rev. C **88**, 045201 (2013); **88**, 049902(A) (2013).
[21] E. Wang, J.-J. Xie, W.-H. Liang, F.-K. Guo, and E. Oset, Phys. Rev. C **95**, 015205 (2017).
[22] J.-J. Xie, L.-S. Geng, and E. Oset, Phys. Rev. D **95**, 034004 (2017).
[23] L. Roca and E. Oset, Phys. Rev. C **95**, 065211 (2017).
[24] V. R. Debastiani, S. Sakai, and E. Oset, Phys. Rev. C **96**, 025201 (2017).
[25] D. Samart, W.-h. Liang, and E. Oset, Phys. Rev. C **96**, 035202 (2017).
[26] S. Sakai, E. Oset, and A. Ramos, Eur. Phys. J. A **54**, 10 (2018).
[27] R. Pavao, S. Sakai, and E. Oset, Eur. Phys. J. C **77**, 599 (2017).
[28] S. Sakai, E. Oset, and W. H. Liang, Phys. Rev. D **96**, 074025 (2017).
[29] J.-J. Xie and F.-K. Guo, Phys. Lett. B **774**, 108 (2017).
[30] M. Bayar, R. Pavao, S. Sakai, and E. Oset, Phys. Rev. C **97**, 035203 (2018).
[31] L. R. Dai, R. Pavao, S. Sakai, and E. Oset, Phys. Rev. D **97**, 116004 (2018).
[32] J.-J. Xie and E. Oset, Phys. Lett. B **792**, 450 (2019).
[33] W.-H. Liang, H.-X. Chen, E. Oset, and E. Wang, Eur. Phys. J. C **79**, 411 (2019).

[34] X.-H. Liu, G. Li, J.-J. Xie, and Q. Zhao, Phys. Rev. D **100**, 054006 (2019).
[35] H.-J. Jing, S. Sakai, F.-K. Guo, and B.-S. Zou, Phys. Rev. D **100**, 114010 (2019).
[36] S. X. Nakamura, Phys. Rev. D **102**, 074004 (2020).
[37] S. Sakai, Phys. Rev. D **101**, 074041 (2020).
[38] R. Molina and E. Oset, Eur. Phys. J. C **80**, 451 (2020).
[39] S. Sakai, E. Oset, and F.-K. Guo, Phys. Rev. D **101**, 054030 (2020).
[40] V. R. Debastiani, S. Sakai, and E. Oset, Eur. Phys. J. C **79**, 69 (2019).
[41] E. Oset and L. Roca, Phys. Lett. B **782**, 332 (2018).
[42] L. R. Dai, Q. X. Yu, and E. Oset, Phys. Rev. D **99**, 016021 (2019).
[43] L. R. Dai, L. Roca, and E. Oset, Phys. Rev. D **99**, 096003 (2019).
[44] V. R. Debastiani, F. Aceti, W.-H. Liang, and E. Oset, Phys. Rev. D **95**, 034015 (2017).
[45] L. Roca, E. Oset, and J. Singh, Phys. Rev. D **72**, 014002 (2005).
[46] M. Lutz and E. Kolomeitsev, Nucl. Phys. **A730**, 392 (2004).
[47] D. Gomez Dumm, A. Pich, and J. Portoles, Phys. Rev. D **69**, 073002 (2004).
[48] M. Wagner and S. Leupold, Phys. Rev. D **78**, 053001 (2008).
[49] D. Dumm, P. Roig, A. Pich, and J. Portoles, Phys. Lett. B **685**, 158 (2010).
[50] X. Zhang and J.-J. Xie, Chin. Phys. C **43**, 064104 (2019).
[51] Q. Huang, C.-W. Shen, and J.-J. Wu, Phys. Rev. D **103**, 016014 (2021).
[52] M. Tanabashi *et al.* (Particle Data Group Collaboration), Phys. Rev. D **98**, 030001 (2018).
[53] M. Ablikim *et al.* (BES Collaboration), Phys. Rev. D **77**, 032005 (2008).
[54] L. S. Geng and E. Oset, Phys. Rev. D **79**, 074009 (2009).
[55] C. Garcia-Recio, L. S. Geng, J. Nieves, and L. L. Salcedo, Phys. Rev. D **83**, 016007 (2011).
[56] P. Zyla *et al.* (Particle Data Group Collaboration), Prog. Theor. Exp. Phys. **2020**, 083C01 (2020).
[57] A. Pich, Rep. Prog. Phys. **58**, 563 (1995).
[58] W.-H. Liang, S. Sakai, J.-J. Xie, and E. Oset, Chin. Phys. C **42**, 044101 (2018).
[59] R. Molina, M. Döring, and E. Oset, Phys. Rev. D **93**, 114004 (2016).